

International Conference on Space Optics—ICSO 2018

Chania, Greece

9–12 October 2018

Edited by Zoran Sodnik, Nikos Karafolas, and Bruno Cugny



End to end calibration of a radiometer at high irradiance levels

Steven van den Berg

Omar El Gawhary

Paul Dekker

Marijn van Veghel

et al.



End to end calibration of a radiometer at high irradiance levels

Steven van den Berg^{*a}, Omar El Gawhary^a, Paul Dekker^a, Marijn van Veghel^a, Ramon Vink^b, Steven Sablerolle^b, Gianluca Casarosa^c

^aVSL, Thijsseweg 11, 2629 JA, Delft, The Netherlands;

^bSERCO BV, Kapteynstraat 1, 2201 BB Noordwijk, The Netherlands;

^cESA-ESTEC, Keplerlaan 1, 2201 AZ Noordwijk, The Netherlands

ABSTRACT

In this contribution we present a method to calibrate a radiometer at high irradiance levels (18 kW/m²). The method has been developed in the frame of the ESA Technology Research Programme. The radiometer under test is used as a reference detector in solar simulators. In order to underpin that the irradiance level that is generated in the solar simulator is within the required levels of uncertainty, the performance of the reference radiometer has been validated. The concept of the calibration of the radiometer is that the radiometer cavity is exposed to a known optical flux, provided by a laser. Taking into account the area of the cavity aperture, which is measured independently with a coordinate measurement machine, the average irradiance level is determined. The reading of the radiometer is then compared to the applied irradiance level. For this calibration the challenge is not only to achieve SI traceability at high irradiance levels, but also to meet other requirements like not to exceed a pre-determined level of irradiance at any position of the radiometer cavity, to avoid potential damage. The measurement uncertainty for the calibration of the instrument is < 1%. Results show that the irradiance provided by the radiometer agrees within the measurement uncertainty with the known applied irradiance over the tested calibration range (0.04 W/cm² - 1.8 W/cm²).

Keywords: radiometer, electrical substitution irradiance, calibration, solar simulator, laser, metrology

1. INTRODUCTION

The European Space Research and Technology Centre (ESTEC) in Noordwijk, the Netherlands, hosts a test centre where environmental tests on small up to large spacecrafts and aerospace structures are performed in dedicated test facilities. The test centre operates three thermal vacuum facilities, and two of them, the Large Space Simulator (LSS) and the Vacuum Thermal Chamber (VTC1.5) are equipped with a sun simulator. The sun simulator is an optical system based on one or more Xenon lamps, needed to illuminate the test article at ambient conditions or in thermal vacuum. The optical flux reaching the test article varies depending on the test and it can be as high as 28 kW/m². The beam generated by the sun simulator is required to be periodically calibrated (e.g. when the lamps are replaced or when the intensity is varied) and this is done by means of a radiometer. Since the radiometer system (a Kendall Mk IV) is used as reference standard for the measurement and characterization of the sun simulator, its calibration plays a key role. SI traceable calibration of the instrument is essential for ensuring the reliability of the irradiance tests. In this paper we discuss the calibration of the reference radiometer for irradiance levels up to 18 kW/m². The calibration method has been developed in the frame of the ESA Technology Research Programme.

Kendall radiometers of type IV are instruments designed to measure high level of total irradiance of sources, with the capability of measuring over broad spectral ranges, from the UV to the IR part of the electromagnetic spectrum [1][4]. This type of radiometers is not only used for sun simulator calibration, it also serves as reference standard for the calibration of heat flux sensors, which have a wide range of applications e.g. in fire research, aerospace and for irradiance measurement of solar concentrators [5-7]. The radiometer operation principle is based on an electrical substitution method to determine the total absorbed power in a black cavity. Electrical substitution calibrated radiometers (ESR) are traceable to SI electrical units via the measurement of electrical power. This requires calibration of the cavity heater resistance and calibrated measurement of the cavity heater voltages or currents. Furthermore, the area of the cavity aperture has to be calibrated to

* svdberg@vsl.nl

be able to determine the irradiance level from the absorbed optical flux. As such, ESRs serve as an absolute standard for the irradiance scale, without further need for calibration. However, to verify or eventually improve the calibration of the radiometer, though self-calibrating, traceability to an absolute cryogenic radiometer can be established [3][8].

In order to calibrate the radiometer for irradiance, it is exposed to a known flux (optical power) from a high-power continuous wave laser, which just underfills the cavity aperture. The area of the radiometer cavity aperture is measured independently through a coordinate measurement machine (CMM). The average irradiance applied to the radiometer is then determined from the optical flux and the aperture area. The main challenge in the calibration are the high irradiance levels required, up to at least 18 kW/m². This requires SI traceable measurement of optical flux up to 1.8 W, which is by three to four orders of magnitude higher than the operation range of commonly available silicon-based reference detectors. Another challenge is the requirement to have a sufficiently high average irradiance over the cavity area to cover the calibration range, while at the same time a) underfilling the cavity, but b) at no point exceeding the maximum irradiance level of 42 kW/m² which is the maximum operation range of the instrument. This requires a near-perfect top-hat beam shape. Several beam-shaping methods have been investigated to approximate this as much as possible. Both the optical power measurement and the aperture measurement are traceable to SI units. The applied optical power is measured with a reference detector traceable to the primary cryogenic radiometer of VSL. The measurements with the CMM are traceable to the SI meter via a calibrated laser interferometer. The measurement method and traceability chain are discussed in section 2. The calibration results are presented in section 3. As discussed in section 4, a relative calibration uncertainty of 0.9% at 95% level of confidence ($k = 2$) is achieved.

2. CALIBRATION METHOD

2.1 Calibration concept and traceability route

The general concept of the calibration of the radiometer is that the radiometer cavity is exposed to a known optical flux, provided by a laser. Considering the area of the cavity aperture, which is measured independently, the average irradiance level is determined. The radiometer reading will be then compared to the applied irradiance. The measurement range is 0.4 kW/m² - 18 kW/m². For a nominal aperture area of 1 cm², this corresponds to an applied laser power of 0.04 W - 1.8 W. The average irradiance level applied to the radiometer will be retrieved from the applied flux and the aperture area, following the basic measurement equation:

$$E = \frac{\Phi}{A}, \quad (1)$$

with E the average irradiance, Φ the incident flux and A the aperture area. The calibration thus breaks down into an optical and a geometrical measurement. The traceability chain is shown in Figure 1. A primary silicon-diode-based trap detector is calibrated against an absolute cryogenic radiometer (ACR), which is based on the same physical principle as the Kendall ESR, but reaches a measurement uncertainty below 0.05%, due to the low temperature of operation (typically 5-10 K) [9]. The responsivity of the trap detector (which is a configuration of 3 photodiodes, 'trapping' the incident radiation) [10], is calibrated against the ACR as a function of wavelength. For this calibration a comparator setup is used, based on a tunable monochromatic source (either a laser or a white light source combined with a double monochromator system) alternatively illuminating the ACR cavity and the trap detector. Similarly, the secondary working standard is calibrated against the primary detector. The final step is to calibrate the radiometer against the secondary standard (called reference detector) using a high-power laser source, having an output power of several Watts. As described in the next paragraph some additional steps are needed here to bridge the gap between the laser power and the maximum power that can be applied to the reference detector.

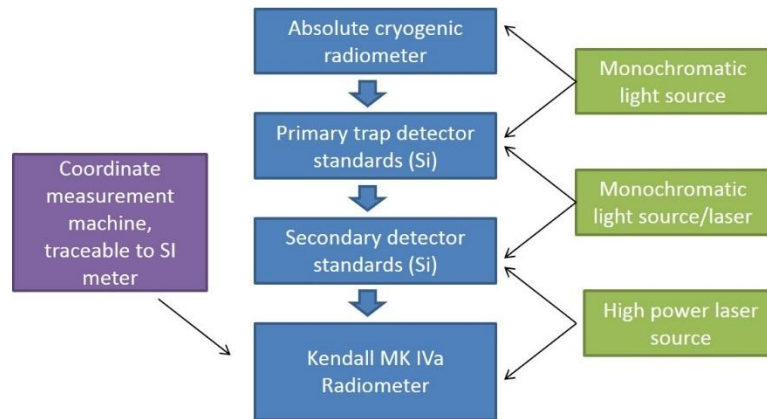


Figure 1. Traceability route for a high-irradiance radiometer to a cryogenic radiometer

2.2 Optical flux calibration

The setup for the optical calibration is shown in Figure 2. First the reference detector responsivity is calibrated against the trap detector. Both detectors are mounted next to each other on a translation stage and exposed to the laser beam that is attenuated to values < 1 mW. The laser source is a diode-pumped solid-state laser, which emits a continuous wave at 532 nm, with a maximum power of 6.5 W. Calibration takes place by measuring the detector currents of both trap and reference detector after each other at various laser powers. Here a monitor detector is used to account for possible power fluctuations of the laser. For this measurement the beam size of the laser is limited to about 4 mm by means of an aperture, to ensure underfilling of the aperture of the trap detector (6 mm diameter).

Since the maximum exposure of the photodiode-based reference detector is limited to an optical power of about 1 mW, direct measurement of the laser power that will be applied to the radiometer (> 1 W) is not possible. In order to bridge this gap, a small fraction (about 10^{-2}) of the laser beam is reflected from a beam splitter and sent to the monitor detector (PD_{mon}). The light propagating towards PD_{mon} is further attenuated with neutral density filters (1.3 dB + 0.6 dB). Both the reference and monitor detector are Si photodiodes with an area of 18×18 mm². The current of each photodiode is amplified with a calibrated trans-impedance amplifier and the resulting output voltage is measured with a calibrated voltmeter. The signals from both PD_{monitor} and PD_{ref} are measured simultaneously and the ratio between these two signals is determined for various power levels. For this measurement the laser beam has been shaped such that it will underfill the aperture of the radiometer, while achieving highest possible flux levels. The ratio between the currents generated by PD_{monitor} and PD_{ref} is about 1.5×10^{-4} . The amplification factor of the transimpedance amplifiers are 10 k Ω and 1 M Ω for the reference and monitor detector, respectively. From this measurement the optical flux at the position of the reference detector is thus linked to the photocurrent of the monitor detector, which we refer to as ‘effective responsivity’.

Subsequently, the radiometer head is mounted on the translation stage instead of the trap detector. Calibration of the radiometer takes place by varying the laser power to values up to 1.8 W. The applied flux to the radiometer is determined from the signal of the monitor detector. Since the photocurrent through the monitor detector is much higher than during its calibration, the amplification factor has been reduced to 10 k Ω . The shape and power control of the laser beam applied to the radiometer is discussed in the next paragraph.

In the calibration procedure described above, the current measured by the monitor detector is changing over a large dynamic range (about 4 orders of magnitude), since the calibration takes place at much lower flux than the actual calibration of the radiometer. As a check whether the detector linearity is sufficient when covering this large dynamic range, the 13 dB attenuator in front of the monitor detector has been calibrated independently. Subsequently the monitor detector was calibrated against the reference in the same way as described above, but without the 13 dB attenuator in the beam, so a larger diode current was generated from the monitor. Then the ‘effective responsivity’ of this two-step approach was calculated from the filter transmission and the calibration of the monitor detector as performed without the filter. The relative difference with the single step approach as described above turns out to be $< 0.1\%$, which underpins that no significant nonlinearity occurs in the single-step approach.

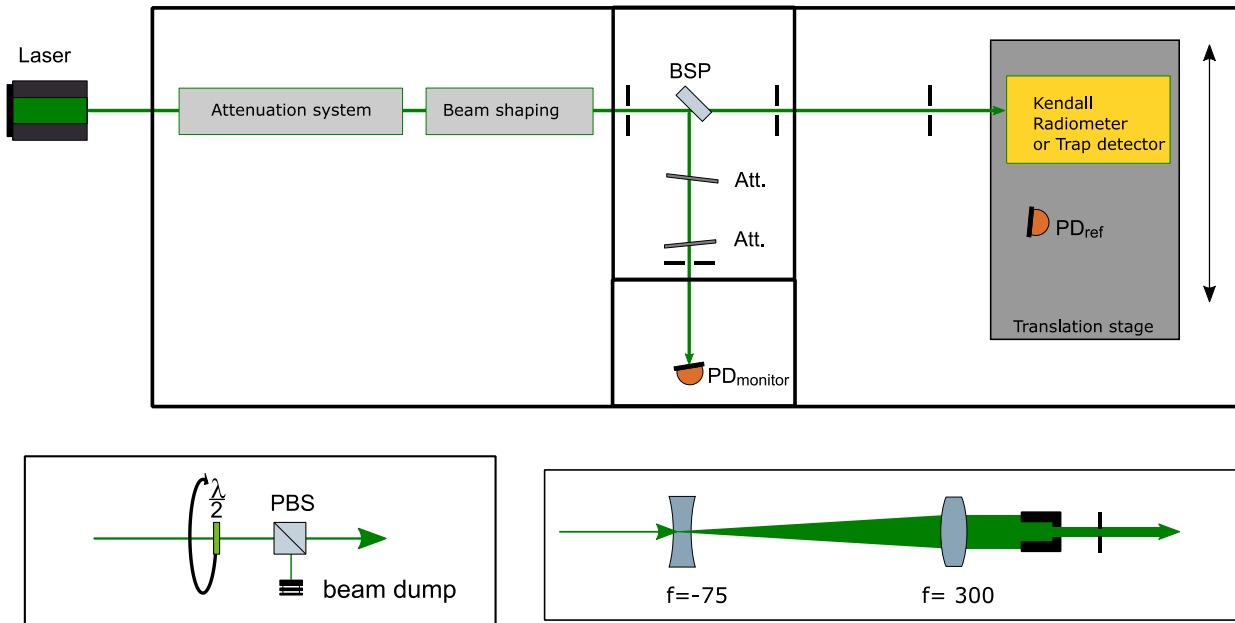


Figure 2. Top: Overview of the setup. A collimated laser beam from a diode-pumped solid-state laser is sent to a variable attenuation system and beam shaping optics. The beam is split into two by a non-polarizing beam splitter (BSP). The reflected beam is attenuated by a 13 and 6 dB optical attenuator. The transmitted beam is sent to a translation stage and is detected by a trap detector, reference detector or the Kendall radiometer. The calibration setup is shielded by a light-tight box that consists of several compartments for stray light suppression. Bottom left: details of the attenuation system, based on a rotating half-waveplate and a polarizer (PBS). Bottom right: configuration of the beam shaping optics, generating a cut-Gaussian beam profile.

2.3 Power control and beam shaping

The optical power is controlled by an attenuation system consisting of a rotatable half-wave plate in combination with a polarizing beam splitter, dividing the total power between the calibration setup and a beam-dump. The half waveplate is used to rotate the polarization, while the polarizer is in a fixed position. This results in a beam with a well-defined and fixed output polarization after the attenuation system and a dynamic range of about 3 orders of magnitude.

One of the challenges of the calibration is to achieve an average irradiance level over the exposed surface of the radiometer as high as possible, while at the same time not exceeding a maximum irradiance level of 42 kW/m² locally. Furthermore, the principle of the calibration requires that all the light that is sent towards the radiometer is reaching the absorbing cavity, i.e. the aperture must be underfilled.

To create a top-hat beam profile, a commercially available beam shaper has been included in the setup and the beam shape was optimized with two additional telescopes (a 2× magnifying telescope in front of the beam-shaper and a 1.5× magnifying telescope after the beam-shaper). With this configuration a top-hat beam with a diameter of 8-9 mm was created. The beam shape was measured with a line-CCD array. A typical shape of the beam profile is shown in Figure 3 (left). The beam profile as obtained with the top-hat beam shaper shows a strong variation of the irradiance level over the beam. To obtain a smoother beam profile an alternative route to shape the beam was investigated, by expanding the Gaussian beam shape and cutting the edges with an aperture (see Figure 2). This was implemented by using a 1:4 telescope for beam expansion and cutting the beam by a 10 mm fixed aperture, followed by a variable aperture set at about 9 mm. With this method a smoother beam profile is obtained, but a large fraction of the laser power is cut (about 45% of the laser power is sent to the radiometer, compared to about 85% for the top-hat profile). It was decided to calibrate the radiometer with this beam profile. To meet the requirement to stay below 42 kW/m², the applied flux was restricted to a maximum value of 1.8 W.

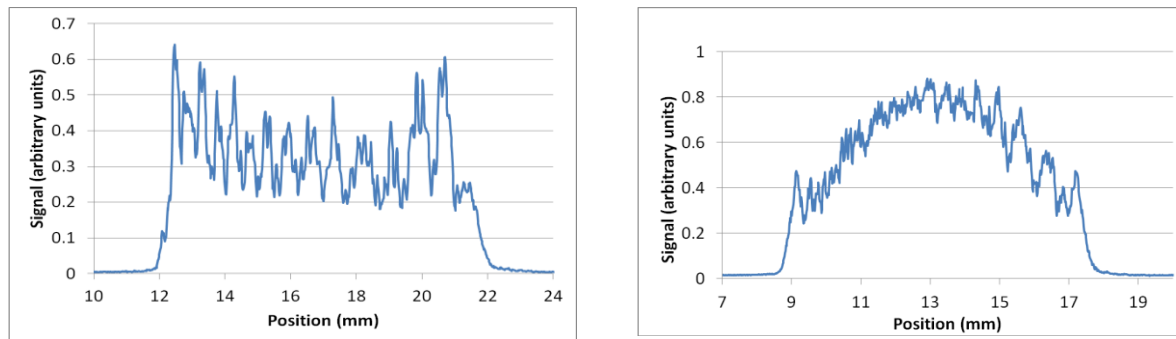


Figure 3. Left: beam profile as measured with the top-hat beam shaper. Right: beam profile as measured with the cut-Gaussian profile.

2.4 Aperture size calibration

The diameter of the radiometer aperture is measured with a coordinate measurement machine, which has a measurement uncertainty $< 1 \mu\text{m}$. The diameter is measured at several positions to estimate the typical diameter variation. From the multiple measurements an average value for the diameter is calculated. The measurement method is contact-based, with a cylindrically shaped probe touching the edge of the aperture. A cylindrical shape is chosen because of the relatively sharp edge of the aperture that needs to be measured. In contrast to a spherical probe a cylindrical probe is much less sensitive to the exact depth of the probe into the aperture. The diameter of the cylindrical probe is 3 mm, which is chosen such that local spatial variations of the cavity aperture can be observed (roundness deviation). The applied force is about 0.2 N. A test was performed on a (relatively soft) aluminum dummy aperture at various levels of probing force, to see if any permanent deformation of the aperture edge was induced. No such deformation could be observed for the force applied in the actual calibration of the radiometer aperture.

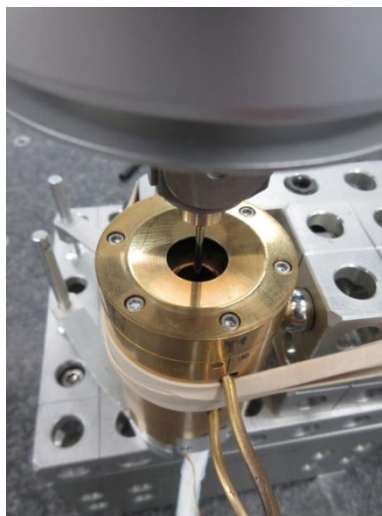


Figure 4: Mounting of the radiometer head on the coordinate measurement machine.

The diameter of the radiometer aperture is found to be (11.2766 ± 0.0025) mm. The measurement uncertainty ($k=2$) includes the deviation of the roundness. The corresponding aperture area is: (0.9987 ± 0.0004) cm². The relative measurement uncertainty of 0.04% is a minor contribution to the uncertainty budget.

3. CALIBRATION RESULTS

The setup for the calibration of the optical power as built, is shown in Figure 5. The setup is shielded by a box, that is subdivided into several compartments to suppress stray light. The radiometer head is connected to a closed water circulation system for temperature stabilization of the radiometer body. The translation stage is equipped with a linear encoder, which allows for the reproducible alignment of the radiometer and the reference detector with respect to the laser beam. By rotating the waveplate of the variable attenuator the flux applied to the radiometer is changed from 47 mW to 1850 mW. Based on the cavity aperture the average irradiance is calculated, according to equation (1). The measurement results are summarized in Table 1 and in fFigure 6. The average deviation of the radiometer is found to be -0.76%, with a standard deviation of 0.06%. More details on the uncertainty budget can be found in the next section.

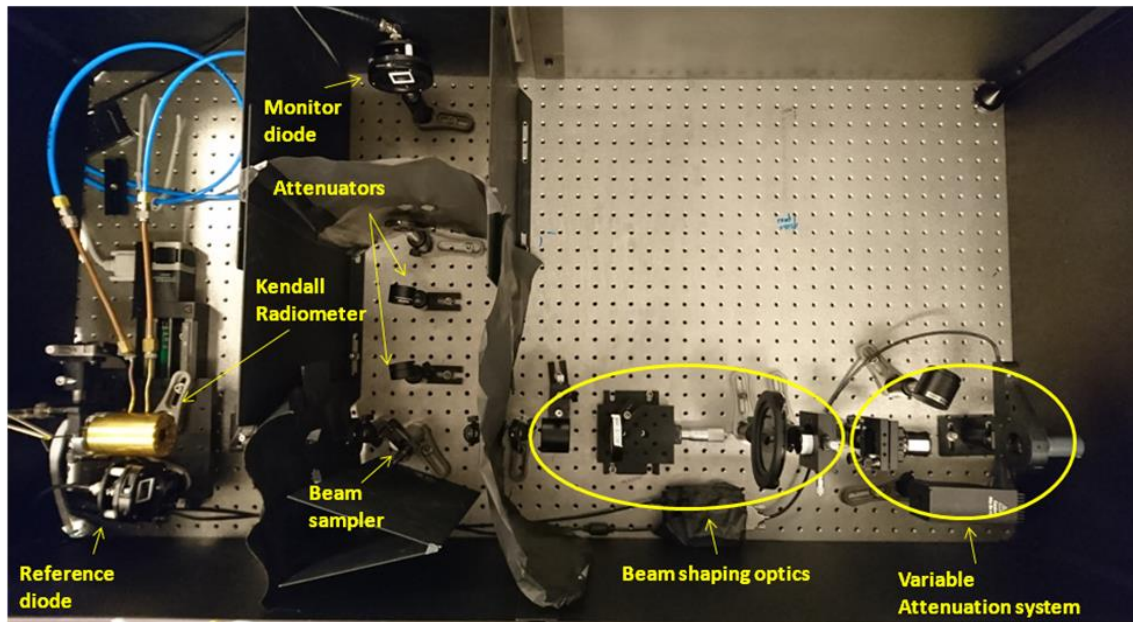


Figure 5. Overview of the setup for the calibration of the radiometer. The laser beam enters the box from the right side, first passing through the attenuation system. The box is divided in several compartments to reduce stray light effects.

Table 1. Calibration results of the radiometer for irradiance levels up to 1.85 W/cm². The average and standard deviation of the relative difference have been calculated without taking into account the first measurement point (to avoid excursions due to the limited resolution of the radiometer).

Applied average irradiance (mW/cm ²)	Radiometer reading (mW/cm ²)	Relative difference (%)
46.9	46.5	-0.83
186.3	185.1	-0.65
363.9	361.4	-0.69
557.6	553.6	-0.71
749.0	743.4	-0.74
906.3	899.8	-0.71
1101.5	1093.3	-0.74
1288.1	1278.2	-0.77
1460.2	1447.7	-0.85
1648.4	1634.7	-0.83
1845.1	1829.3	-0.86

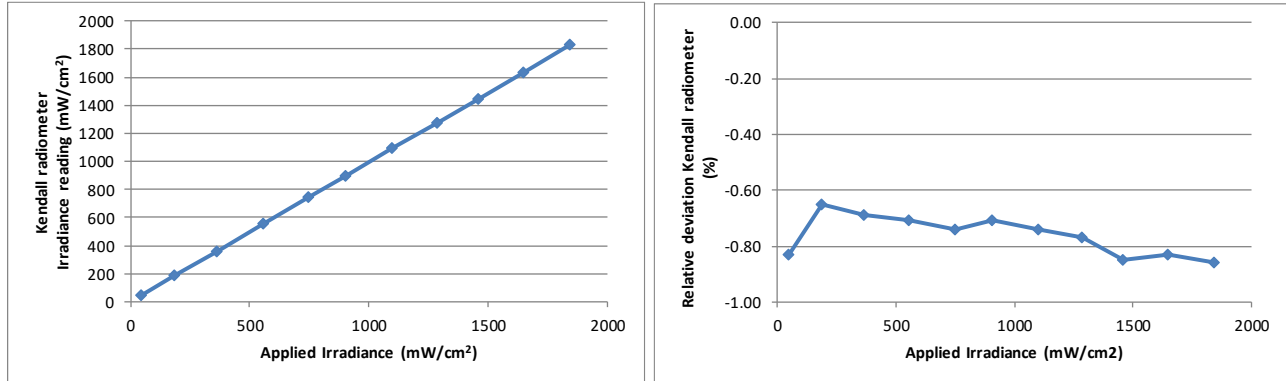


Figure 6. Left panel: radiometer reading versus applied average irradiance. Right panel: relative difference between applied irradiance and measured irradiance as measured by the radiometer.

The short-term reproducibility has been investigated by performing two calibration series directly after each other, with about 1 hour in between. These measurements are in agreement and show a reproducibility of the results within 0.1%. The medium-term stability and reproducibility of the method has been investigated by repeating the measurement about 4 weeks later. Several changes to the setup have been made (realignment, slight modifications to improve the beam quality) compared to the first series. Furthermore, the radiometer has been shipped to ESA ESTEC and back to VSL between the two measurement series. The second measurement series shows very similar results with a deviation of -0.73% with a standard deviation of 0.04%. The difference between both measurement series is thus far below 0.1%. No measurable drift on this time-scale is observed.

4. UNCERTAINTY BUDGET

The response of the radiometer under test R_K is defined as its read value ($S_{reading}$, in V) divided by the applied irradiance.

$$R_K = \frac{S_{reading}}{\Phi} A \tag{2}$$

Here the applied flux is given by

$$\Phi = \frac{I_{monitor}}{m}, \tag{3}$$

With m the ‘effective responsivity’, i.e. the ratio between the flux at the position of the radiometer and the monitor diode current. The response of the radiometer can then be written as:

$$R_K = \frac{S_{reading}}{I_{monitor}} m A \tag{4}$$

A summary table with an uncertainty budget for the calibration of the radiometer is given in

Table 2. The uncertainty on m is based on several other uncertainty contributions, like the uncertainty from the reference detector, transimpedance amplifiers and voltmeter. In addition, uncertainty contributions arising from beam geometry and repeatability have been taken into account, too. The uncertainty due to geometry is associated to the shape of the beam. From measurements with both beam shapes (see Figure 3), it was found that the response of the radiometer slightly depends on the offered beam shape. Possibly, inhomogeneous illumination of the absorptive cavity has a slight impact on the radiometer response. A standard uncertainty contribution of 0.4% was estimated to account for beam geometry. The effect of beam geometry and why this slightly influences the radiometer response, could be a topic for further investigations.

Table 2. Uncertainty budget

Variable	Description	Value		Uncertainty		Coverage factor k	Standard uncertainty	Sensitivity coeff.	u(R _k)	
S _{reading}	Radiometer reading	1.8	V	1.80E-04	V	1	1.80E-04	0.555	9.99E-05	$\frac{V}{m^2/W}$
A	Aperture area	0.998726	cm ²	2.22E-04	cm ²	1	2.22E-04	1	2.22E-04	$\frac{V}{m^2/W}$
I _{monitor}	Current monitor detector	7.79E-05	A	1.10E-08	A	1	1.10E-08	1.28E+04	1.41E-04	$\frac{V}{m^2/W}$
m	'Effective responsivity'	4.227E-05	A/W	3.59E-08	A/W	1	3.59E-08	2.36E+04	8.49E-04	$\frac{V}{m^2/W}$
reprod.	Measurement reproducibility	0.998726	$V m^2/W$	9.99E-04	$V m^2/W$	1	9.99E-04	1	9.99E-04	$\frac{V}{m^2/W}$
geo.	Geometric effects	0.998726	$V m^2/W$	3.99E-03	$V m^2/W$	1	3.99E-03	1	3.99E-03	$\frac{V}{m^2/W}$
R _k	Radiometer response	0.998726	$V m^2/W$					standard uncertainty	0.00421	$\frac{V}{m^2/W}$
								expanded uncertainty	0.00843	$\frac{V}{m^2/W}$
								relative uncertainty	0.42	%
								relative uncertainty	0.9	%

5. CONCLUSION

We have described the calibration of a radiometer at high irradiance levels. The two main ingredients of the calibration approach are a geometrical calibration of the aperture area and the calibration of the radiometer response to a known optical power, while underfilling the aperture. The traceability route for the optical power involves several comparison steps with intermediate standards, providing traceability to the Absolute Cryogenic radiometer (ACR), which is the primary detector standard for radiometry. One challenge was to bridge the gap between the low power operation of the reference standards and the high power operation of the radiometer. A second challenge was to underfill the radiometer cavity in combination with a homogeneous illumination of the cavity. The latter is needed to obtain high average irradiance levels without exceeding a maximum allowed irradiance level locally. The average deviation over the radiometer over the calibration range was -0.7%. The relative calibration uncertainty at 95% level of confidence (k = 2) was 0.9%, dominated by geometrical effects connected to the distribution of light over the cavity, which may be a topic of further research. The short- and mid-term reproducibility of the radiometer have been investigated. A high degree of repeatability, within 0.1%, on the short (hour) and medium (~4 weeks) timescale was observed.

ACKNOWLEDGEMENTS

We like to acknowledge Petro Sonin (VSL) for fruitful technical discussions and for his contribution to the automation of the measurement setup.

REFERENCES

- [1] Kendall, J. M., Berdahl, C. M., "Two blackbody radiometers of high accuracy", *Appl. Opt.* 9, 1082-1091 (1969).
- [2] Wilson, R. C., "Active cavity radiometer type IV", *Appl. Opt.* 18, 179-188 (1979).
- [3] Tsai, B. K., Gibson, C. E., Murthy, A. V., Early, E. A., Dewityt, D. P., Saunders, R. D., "Heat flux sensor calibration", NIST special publication, 250-65 (2004).
- [4] Kostkowski, H. J. [Reliable Spectroradiometry], Spectroradiometry Consulting, La Plata, Maryland (1997).
- [5] Ballestrín, J., Estrada, C. A., Rodríguez-Alonso, M., Pérez-Rábago, C., Langley, L. W. and Barnes, A., "Heat flux sensors: calorimeters or radiometers?", *Solar Energy* 80, 1314-1320 (2006).
- [6] Ballestrín, J., Ulmer, S., Morales, A., Barnes, A., Langley, L.W. and Rodríguez, M., "Systematic error in the measurement of very high solar irradiance", *Solar Energy Materials & Solar Cells* 80, 375-381 (2003).
- [7] Murthy, A. V., Tsai, B. K. and Saunders, R. D., "Radiative calibration of heat-flux sensors at NIST: facilities and techniques", *J. Res. Nat. Inst. Stand. Technol.* 105, 293-305 (2000).
- [8] Murthy, A. V., Tsai, B. K. and Saunders, R. D., "High-heat-flux sensor calibration using black-body radiation", *Metrologia* 35, 501-504 (1998).
- [9] Schrama, C. A., Bosma, R., Gibb, K., Reijn, H. and Bloembergen, P., "Comparison of monochromator-based and laser-based cryogenic radiometry", *Metrologia* 35(4), 431-435 (1998).
- [10] Fox, N. P., "Trap detectors and their properties", *Metrologia* 28, 197-202 (1991).